THE JOURNAL OF PHYSICAL CHEMISTRY A

Article

pubs.acs.org/JPCA

On the Formation of (Anionic) Excited Helium Dimers in Helium Droplets

Stefan E. Huber† and Andreas Mauracher*

Institut für Ionenphysik und Angewandte Physik, Leopold-Franzens-Universität Innsbruck, Technikerstraße 25, A-6020 Innsbruck, Austria

ABSTRACT: Metastable atomic and molecular helium anions exhibiting high-spin quartet configurations can be produced in helium droplets via electron impact. Their lifetimes allow detection in mass spectrometric experiments. Formation of atomic helium anions comprises collision-induced excitation of ground state helium and concomitant electron capture. Yet the formation of molecular helium anions in helium droplets has been an unresolved issue. In this work, we explore the interaction of excited helium atoms exhibiting high-spin triplet configurations with ground state helium using the equation-of-motion coupled-cluster method. Transition barriers in the energetically lowest He*−He and He*$^-$−He interaction potentials prevent molecule formation at the extremely low temperatures present in helium droplets. In contrast, some excited states allow a barrier-free formation of molecular helium (anions). Moreover, we show that the necessary excitation energies pinpoint (higher) resonances in recently recorded mass spectra and emend the assignment of those resonances that have previously been assigned to electron-impact ionization of ground state helium necessitating subsequent double-electron capture. Embedding molecules or molecular clusters in helium droplets is a predestined experimental technique for the study of phenomena at very low temperatures. Profound knowledge about active processes in the helium environment is required for a proper assessment of experimental data.

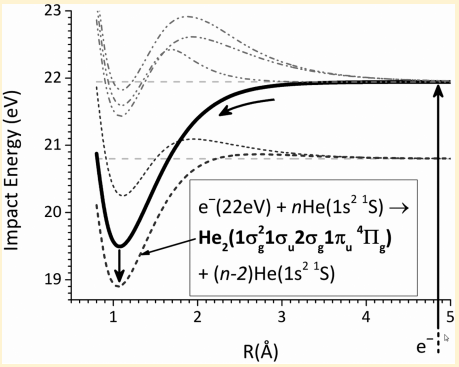

1. INTRODUCTION

Helium droplets provide a unique environment for the study of atoms and molecules at very low temperatures and have thus received substantial attention over the past decade.[1−5] Very low temperatures not only allow explicit investigation of quantum mechanical phenomena but also have advantages for spectroscopic studies such as reducing spectral congestion, sharpening lines as well as simplifying the spectral assignment process. Moreover, experiments at very low temperatures make it possible to explore metastable short-lived species that often yield at best only a fleeting existence at room temperature. Utilization of low temperature experiments can result in detailed information about free radicals, molecular ions, and weakly bound clusters of molecules.[5]

A specialty of helium droplets is their ability to self-adjust their temperature by evaporative cooling. Although the temperature in bulk liquid helium can be continuously adjusted using refrigeration techniques, a helium droplet with a temperature above its steady state temperature of 0.37 K[5] will easily get rid of the excess energy by evaporation of helium atoms. This equilibration is expected to be a very fast process due to the exceptionally high heat conductivity of the superfluid phase of helium, i.e., below 2.18 K,[6] and because of the very weak dispersion forces between (ground state) helium atoms yielding an He−He binding energy of 11 K (about 7.65 cm^{-1} or 0.95 meV).[7] Doping of a helium droplet with a foreign (closed-shell) molecule thus leads to a fast cooling of the dopant to 0.37 K. In addition, due to the exceptionally low viscosity of the superfluid helium phase, translation and rotation abilities of the dopant are much less affected than in other solvents.[5] Moreover, helium droplets are an ideal matrix for spectroscopic studies due to optical transparency ranging from the far IR to the vacuum UV.[1,2,4] Note that the above-mentioned properties of helium droplets apply only to ^{4}He droplets and are different for the case of ^{3}He droplets. However, ^{3}He has a natural abundance that is about 10^6 times lower than that of ^{4}He and shall not be discussed here.

One fundamental question in low-temperature ion physics, which is of specific importance here, is how charges are transported in helium droplets.[8,9] After the discovery of superfluid-like charge transport in helium droplets in 1969,[10] there has been speculation that, in addition to free electrons localized in large 9−15 Å radius bubbles,[11] atomic and molecular helium anions might be important charge carriers. These anions are well-known in the gas phase and have been studied from both experimental[12−14] and theoretical side.[15−20] The basis for the above-mentioned speculation about the relevance of these anions has been observations[21,22] of negative ion resonances upon electron impact on helium droplets at about 22 eV and multiples thereof. This could be brought in

Special Issue: Franco Gianturco Festschrift

Received: April 14, 2014
Revised: May 26, 2014
Published: May 27, 2014

   dx.doi.org/10.1021/jp503643r | J. Phys. Chem. A 2014, 118, 6642−6647

line with the excitation of ground state helium into the first excited triplet state, i.e., He(1s2s ^{3}S),[23] by taking into account the energy loss of the impact electron due to the intrusion into the helium droplet.[24] Recently, dynamic differences between atomic and molecular helium anions, concerning both the interaction with the helium droplet environment as well as possible charge transfer to dopants, have also been discussed to ample extent.[23] Mass spectrometric studies to reveal direct evidence for the formation of both atomic and molecular helium anions in helium droplets are currently being conducted.[25]

The knowledge about expected properties of the two anion species in the helium droplet environment, compiled in an earlier work,[23] is graphically summarized in Figure 1. A solvated

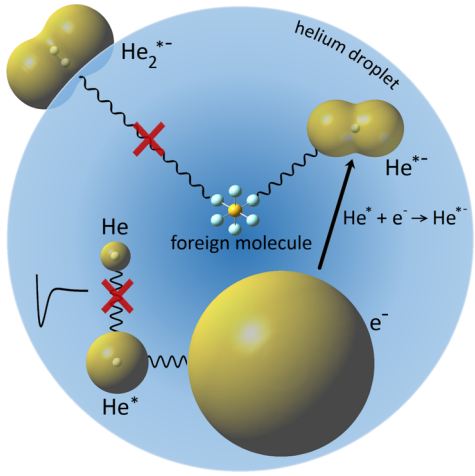

Figure 1. Graphical summary of properties of atomic and molecular helium in helium droplets. The barrier prohibiting the formation of He_2* from He* and He is indicated on the lower left. The formation of He*$^-$ due to attachment of a solvated electron to He* is shown on the right. The interaction of He*$^-$ with a foreign molecule (here: SF_6) embedded in the helium droplet is allowed (upper right). In contrast, He_2*$^-$ is located on the surface of the helium droplet (upper left) and thus the interaction with an embedded molecule is strongly suppressed. The depicted species are to scale, except the size of the helium droplet.

electron can be formed in helium droplets at an energy of about 1.2 eV,[26] forming a very large bubble inside the droplet, schematically depicted in Figure 1. For an impact energy of about 21 eV, the electron can first excite a helium atom into a He(1s2s ^{3}S) state requiring 19.8 eV[27] and subsequently be captured by it to form He(1s2s2p ^{4}P) (also denoted simply as He*$^-$), which is energetically just below the neutral He(1s2s ^{3}S) state (also denoted simply as He*) by 77.1 meV.[28] The atomic anion is both bound and mobile in the helium droplet and thus free to interact with any existing dopants,[23] denoted as "foreign molecule" in Figure 1. Both He(1s2s ^{3}S) and He(1s2s2p ^{4}P) cannot form molecular helium at the droplet temperature of 0.37 K due to the small but existing barriers of 120 and 85 meV, respectively, in the diatomic interaction potentials indicated in Figure 1.[23] It has been speculated that the formation of molecular helium anions requires excitation of ground state helium into higher excited states. This is also due to the fact that the energetically lowest resonance associated with He_2^{*-} ($\triangleq$ $He_2(1\sigma_g^2 1\sigma_u 2\sigma_g 1\pi_u\ ^4\Pi_g)$) appears at 22.9 eV.[23] Another formation pathway well-known for the production of molecular helium anions is electron impact ionization of helium at 24.5 eV, resulting in He^+ allowing a barrier-free formation of He_2^+ and subsequent double electron transfer from laser excited alkali metals.[29] An analogous process, i.e., the formation of He^+ and He_2^+ with a subsequent two-electron capture, has been predicted in helium droplets for an initial electron impact energy of about 25.5−26.5 eV.[23] This energy is, however, somewhat too high regarding previously reported higher ion resonances.[23] All the ion resonances and assumed formation pathways discussed earlier[23] are summarized in Table 1. Once

Table 1. Ion Resonances and Assigned Formation Pathways for Associated Ions As Reported Previously[23] [a]

anion	energy (eV)	formation pathway
He*$^-$	22.0 ± 0.2 (exp)	$e^- + He \rightarrow e^- + He^* \rightarrow He^{*-}$
He*$^-$	23.0 ± 0.2 (exp)	possibly: $e^- + He \rightarrow e^- + He^{**} \rightarrow He^{*-}$
He*$^-$	25.1 ± 0.5 (exp)	possibly: $e^- + He \rightarrow e^- + He^{***} \rightarrow He^{*-}$
He*$^-$	25.5−26.5 (th)	$e^- + He \rightarrow 2e^- + He^+ \rightarrow He^{*-}$
He_2*$^-$	22.9 ± 0.2 (exp)	possibly: $e^- + 2He \rightarrow e^- + He^{**} + He \rightarrow e^- + He_2^* \rightarrow He_2^{*-}$
He_2*$^-$	24.8 ± 0.5 (exp)	possibly: $e^- + 2He \rightarrow e^- + He^{***} + He \rightarrow e^- + He_2^* \rightarrow He_2^{*-}$
He_2*$^-$	25.5−26.5 (th)	$e^- + 2He \rightarrow 2e^- + He^+ + He \rightarrow 2e^- + He_2^+ \rightarrow He_2^{*-}$

[a] Several asterisks indicate involvement of higher excited states. Energy values are taken from either experiment (exp) or theory (th).

formed, the molecular helium anion has been shown not to be bound inside liquid helium and to reside at the surface of helium droplets leading to substantial suppression of any charge transfer from this anion to embedded dopants.[23] However, beyond mere speculation, the underlying principles leading to the formation of molecular helium anions as well as the higher ion resonances collected in Table 1 are an open issue yet. The latter shall be tackled in the present study by a quantum chemical exploration of a series of excited helium states and associated diatomic interaction potentials.

2. METHOD

Excited states were calculated using the equation-of-motion coupled cluster with single and double substitions (EOM-CCSD) approach.[30] To retrieve diatomic interaction potentials, we varied the distance between two helium nuclei in a range 0.8−10.0 Å. The reference state was chosen as the He (or He_2) ground state, i.e., He(1s^2 ^{1}S) (or $He_2(1\sigma_g^2 1\sigma_u^2\ ^1\Sigma_g^+)$), whereas the target states were the energetically lowest excited triplet states. The large HOMO−LUMO gap of the spin-restricted reference results in a single-configurational ground state and low-lying excited states that are of singly excited character. This choice guarantees a reasonable description of the excited states. In contrast, the He_2*$^-$ state, i.e., $He_2(1\sigma_g^2 1\sigma_u 2\sigma_g 1\pi_u\ ^4\Pi_g)$, is of considerable multiconfigurational character, reflected in a value of about 0.2 employing the T1 diagnostic of Lee and Taylor,[31] and does thus not serve as a reliable reference state for the calculation of excited anionic states. The latter is also true for the significantly lower-lying doublet anion state, however, this time due to the fact that the excess electron is not bound to the neutral He core. For these reasons, we did not calculate any excited states of the molecular helium anion.

We employed the quadruply augmented cc-pVQZ basis set as defined in an earlier work.[23] For short, we shall call it q-aug-cc-pVQZ in the following, although it deviates slightly from the homonymous basis set defined by Woon and Dunning.[32] In particular, the exponents of the diffuse functions beyond second

dx.doi.org/10.1021/jp503643r | J. Phys. Chem. A 2014, 118, 6642−6647

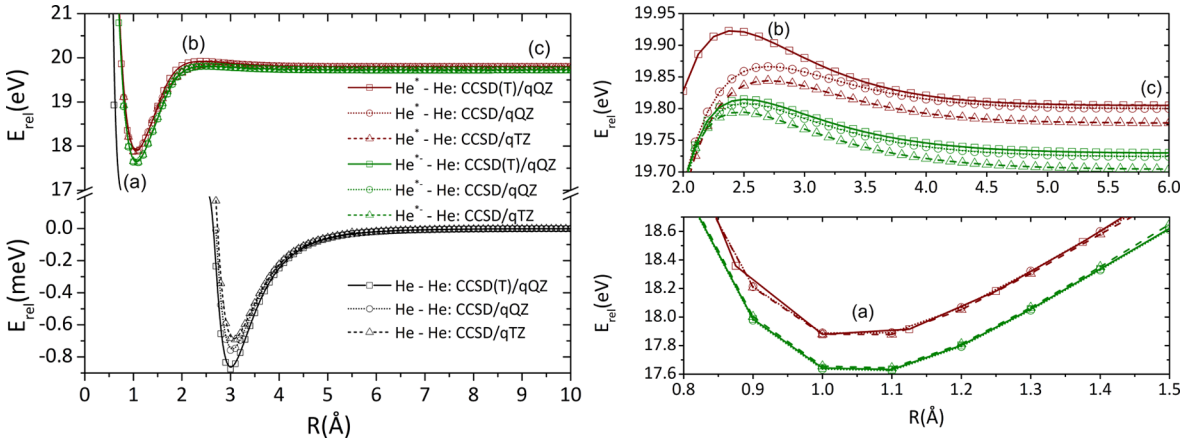

Figure 2. Potential energy scans for the neutral systems He(^{1}S)−He(^{1}S) (black) and He(^{3}S)−He(^{1}S) (wine red) and the anionic system He(^{4}P)−He(^{1}S) (olive green) derived at CCSD(T)/q-aug-cc-pVQZ (squares; short notation for basis, qQZ), CCSD/q-aug-cc-pVQZ (circles), and CCSD/q-aug-cc-pVTZ (triangles; short notation for basis, qTZ). In the right upper and lower panel magnifications of the barrier and long-range regions ((b) and (c)) as well as the minima (a) for the interaction potentials are depicted.

least diffuse ones are obtained by global scaling with a factor of 1/3 instead of the angular-momentum dependent scaling factors used by Woon and Dunning.[32] We found that this choice of basis leads to a considerably better convergence behavior, especially concerning the convergence of the SCF iterations, whereas the obtained energies, geometries, and orbitals are only insignificantly affected. The calculations have been performed using the Gaussian 09 suite of programs[33] and the QChem 3.1 software package.[34] All interaction potentials have been corrected for the basis set superposition error.

Conservatively, the accuracy of EOM-CCSD is estimated to be within 0.1−0.3 eV,[35] whereas the relative spacing of excited states is obtained more accurately.[36] Concerning the present application, we note that we obtained 19.80 eV for the excitation energy corresponding to the lowest lying excited atomic state of helium, i.e., He(1s2s ^{3}S), in very good agreement with the experimental value of 19.82 eV.[27] The electron affinity of this state (with respect to the lowest lying metastable atomic anion in the 1s2s2p ^{4}P configuration) yields 73.8 meV, which is only slightly lower than the 74.9 meV obtained earlier at the CCSD(T)/q-aug-cc-pVQZ level of theory[23] and also in very good agreement with a high-level theoretical estimate of 77.1 meV.[28] In Figure 2, we compare the ground state He−He, the first excited triplet He*−He and the lowest lying excited quartet He*$^-$−He interaction potentials as obtained at the (EOM-)CCSD/q-aug-cc-pVQZ level of theory with results from an earlier study at the CCSD(T)/q-aug-cc-pVQZ level of theory.[23] To get a notion of the effect of basis set size, we depict also the respective curves obtained at the CCSD/q-aug-cc-pVTZ level of theory (with the basis set being the triple-ζ analogue to the quadruple-ζ basis set introduced above). The energy scale is chosen such that the energy of a single helium atom in its ground state corresponds to zero.

We note that the agreement between the three employed levels of theory is very good, within 0.2 meV concerning the reference ground state He−He interaction potential. In the case of the excited neutral and anionic interaction potentials, the agreement is generally in the range of a few tens of millielectronvolts. By decomposition of the interaction potential into three regions, i.e., (a) the potential minima, (b) the barriers, and (c) the long-range part, we point out the following: The accordance between the three considered levels of theory is within 10−15 meV in the region of the potential minima, whereas the inclusion of noniterative triples accounts for about 5−10 meV. In the region of the barriers, the CCSD method underestimates the barrier heights for both neutral and anionic excited configurations. In the case of the He*−He interaction potential, CCSD yields heights about 50 and 80 meV too low (taking the CCSD(T)/q-aug-cc-pVQZ as reference) for the quadruple- and triple-ζ basis sets, respectively. In the case of the He*$^-$−He interaction potential, the agreement is better, and the heights are only underestimated by about 5 and 15 meV, respectively. In the long-range part of the interaction potentials, the results obtained with CCSD using the quadruple- and triple-ζ basis set are about 5 and 25 meV, respectively, lower than the CCSD(T)/q-aug-cc-pVQZ results. Altogether, we note that basis set truncation results in an accuracy of about 30 meV, whereas the inclusion of noniterative triples can account for up to 50 meV. Thus, the accuracy of our approach is estimated to be at least within about 80 meV (and rather too low than too high) in the barrier region and substantially better (within about 25 meV) apart from it. Nonetheless, trends such as relative barrier heights might be reproduced more accurate.

3. RESULTS AND DISCUSSION

As outlined in the Introduction the formation of He_2*, i.e., $He_2(1\sigma_g^2 1\sigma_u 2\sigma_g\ ^3\Sigma_u^+)$, from two helium atoms via excitation of He($1s^2\ ^1$S) into He(1s2s ^{3}S) for one of the atoms is prevented by a transition barrier in the interaction potential, apparent from Figure 2. In a recent study it has been shown that the presence of the barrier is accompanied by a substantial deformation of the 2s orbital of He(1s2s ^{3}S), whereas core orbitals are substantially less affected.[23] It has been suggested that excitation into energetically higher triplet configurations than He(1s2s ^{3}S) such as He(1s2p ^{3}P) might allow a barrier-free molecule formation. This suggestion appears adequate due to the following considerations.

Let two helium atoms be aligned along the *x*-axis, one in its ground state and the other in the He(1s2s ^{3}S) configuration. For large distances between them, the energy will be given simply by the excitation energy required to form He(1s2s ^{3}S) if the energy of ground state He($1s^2\ ^1$S) is defined to be zero. However, if the helium atoms are brought closer to each other,

dx.doi.org/10.1021/jp503643r | J. Phys. Chem. A 2014, 118, 6642−6647

the energy will begin to rise due to the increasing overlap of the involved orbitals, Figure 3a, which gives rise to a large Coulomb integral.

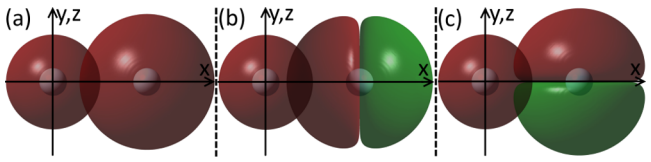

Figure 3. Schematics of the overlap of involved atomic orbitals demonstrating the deliberation concerning the influence of symmetry on the Coulomb integral: (a) 1s−2s, (b) 1s−2p_x, and (c) 1s−2p_z. In contrast to (a) and (b) the Coulomb integral for (c) is expected to be essentially zero, which suggests that there is no barrier for dimer formation when one electron is excited into a p-orbital perpendicular to the molecular axis.

Let now the excited helium atom correspond to He(1s2p ^{3}P) instead. For very large distances between the atoms, the latter excited configuration is 3-fold degenerate as occupation of each of the 2p_x, 2p_y, and 2p_z orbitals gives rise to the same energy. Bringing the atoms together is expected to lift this degeneracy because the overlap between the 2p_x orbital of the excited helium atom and the 1s orbital of the ground state helium leads to a rise in energy for the same reasons as outlined above, Figure 3b. However, the occupation of a 2p orbital perpendicular to the molecular axis results in vanishing overlap. The 2p orbitals perpendicular to the molecular axis exhibit a nodal plane including the molecular axis, and the contributions due to overlap are the same in magnitude above and below the plane, and thus they cancel, Figure 3c. Although the Coulomb integral does not necessarily vanish in case of a vanishing overlap, it can be assumed to be considerably smaller than for occupation of the 2p_x orbital, as discussed before. Intuitively, a vanishing barrier for occupation of a 2p orbital perpendicular to the molecular axis might be expected. These considerations are, however, based on the assumption that at least the reflection properties of the (initially atomic) orbitals with respect to their nodal surface are retained upon approach of the helium atoms toward each other.

Thus, we tested this simple picture by calculating interaction potentials between the lowest lying excited triplet configurations of helium and ground state helium. The results are depicted in Figure 4. The interaction potential associated with ground state helium and He(1s2s ^{3}S) splits into two channels when the He_2* molecule is formed according to occupation of either a bonding σ orbital or an antibonding σ* orbital by the excited electron. The interaction potential associated with the σ* orbital exhibits a substantially higher barrier than the one associated with the σ orbital, Figure 4. This is the case for all interaction potentials under consideration. However, the interaction potentials associated with excitation of an electron into a p-orbital yield a vanishing barrier indeed, given that the bonding π orbital is occupied upon molecule formation, Figure 4. In contrast, occupation of the antibonding π* orbital results in barriers, but somewhat lower than those associated with σ and σ* orbitals stemming from the excitation into a p_x orbital. In general, the barrier heights decrease with increasing principal quantum number, as can be seen by comparison of, e.g., the interaction potentials associated with He(1s2s ^{3}S) and He(1s3s ^{3}S), Figure 4. All barriers for all the interaction channels under consideration are summarized in Table 2.

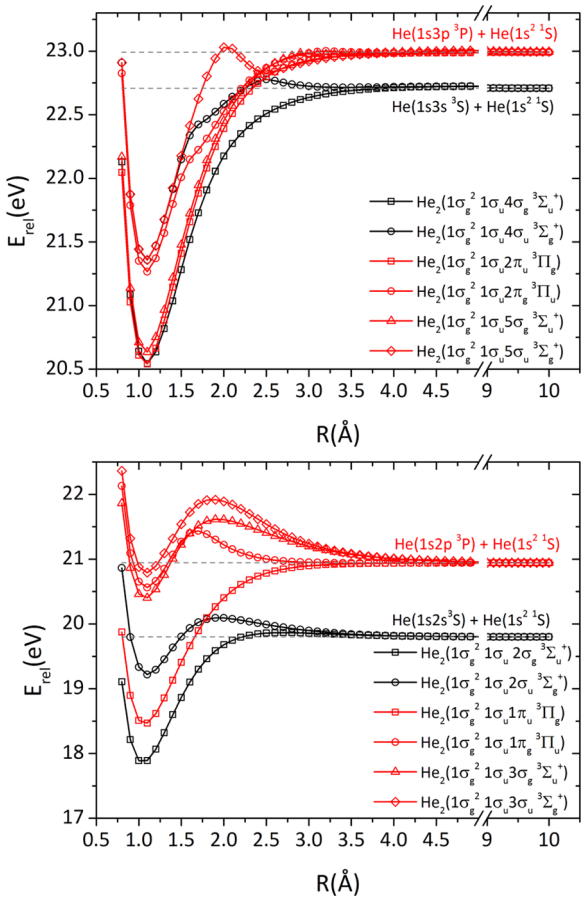

Figure 4. He−He interaction potentials for various excited triplet states. The respective dissociation energies are indicated by gray dashed lines as well as the respective, atomic dissociation configurations. Note that there are no barriers for the configurations $He_2(1\sigma_g^2 1\sigma_u 1\pi_u\ ^3\Pi_g)$ and $He_2(1\sigma_g^2 1\sigma_u 2\pi_u\ ^3\Pi_g)$ upon dissociation.

Table 2. Barrier Heights for All Interaction Potentials under Consideration[a]

atomic configurations	atomic excitation energy (eV)	molecular configurations	barrier height (meV)	degeneracy
He(1s2s ^{3}S) + He(1s^2 ^{1}S)	19.8	$He_2(1\sigma_g^2 1\sigma_u 2\sigma_g\ ^3\Sigma_u^+)$	66	1
		$He_2(1\sigma_g^2 1\sigma_u 2\sigma_u\ ^3\Sigma_g^+)$	294	1
He(1s2p ^{3}P) + He(1s^2 ^{1}S)	20.9	$He_2(1\sigma_g^2 1\sigma_u 2\sigma_u\ ^3\Pi_g)$	0	2
		$He_2(1\sigma_g^2 1\sigma_u 1\pi_g\ ^3\Pi_u)$	500	2
		$He_2(1\sigma_g^2 1\sigma_u 3\sigma_g\ ^3\Sigma_u^+)$	680	1
		$He_2(1\sigma_g^2 1\sigma_u 3\sigma_u\ ^3\Sigma_g^+)$	980	1
He(1s3s ^{3}S) + He(1s^2 ^{1}S)	22.7	$He_2(1\sigma_g^2 1\sigma_u 4\sigma_g\ ^3\Sigma_u^+)$	16	1
		$He_2(1\sigma_g^2 1\sigma_u 4\sigma_u\ ^3\Sigma_g^+)$	72	1
He(1s3p ^{3}P) + He(1s^2 ^{1}S)	23.0	$He_2(1\sigma_g^2 1\sigma_u 2\pi_u\ ^3\Pi_g)$	0	2
		$He_2(1\sigma_g^2 1\sigma_u 2\pi_g\ ^3\Pi_u)$	12	2
		$He_2(1\sigma_g^2 1\sigma_u 5\sigma_g\ ^3\Sigma_u^+)$	19	1
		$He_2(1\sigma_g^2 1\sigma_u 5\sigma_u\ ^3\Sigma_g^+)$	39	1

[a]Atomic and molecular configurations correspond to the electronic states involved at long and short nuclei separation distance, respectively. Degeneracies are also given for the sake of completeness.

dx.doi.org/10.1021/jp503643r | J. Phys. Chem. A 2014, 118, 6642−6647

Although the barriers are generally accounting only for a few tens of millielectronvolts, they are expected to prevent He_2* formation entirely at the very low temperatures present in helium droplets. To get a taste of the unlikeliness of overcoming said barriers, we assume the velocities of the helium atoms obey a Boltzmann distribution and calculate the probability of a helium atom to exhibit a higher kinetic energy than the barrier height. Due to the very weak interaction between ground state helium atoms and the extraordinary speed of thermal equilibration in superfluid helium,[1] this is a reasonable assumption at least as long as the excess energy deposited in the helium droplet is small. Small energies imply here a negligible change in the droplet size upon evaporative cooling. We note that the calculated probabilities are virtually zero at 0.37 K, i.e., below 10^{-164}, and also several K above, i.e., at 10 K the probability is below 4×10^{-6}. The given values correspond to the smallest barrier height, Table 2. Thus, we believe that virtually no helium atom can acquire enough kinetic energy to classically overcome any of the nonzero barriers.

Thus, only two (2-fold degenerate) channels remain for the formation of He_2*, i.e., the ones associated with excitation into 2p and 3p orbitals perpendicular to the interatomic axis. The corresponding excitation energies read 20.9 and 23.0 eV. We note that the excitation energy for He^{*-} corresponding to $He(1s2p^2)$ is above yielding 21.0 eV. On the basis of the foregoing discussion, this state is expected to yield a vanishing barrier too. However, it is unstable toward the formation of neutral He(1s2p) and a free electron in contrast to the lowest excited helium state, which has a small yet nonzero electron affinity. Taking into account the energy needed to penetrate the helium droplet, i.e., 1−2 eV,[24] we suggest the following formation pathways including intermediated excited states for atomic and molecular helium anions in helium droplets (with appearance energies in parentheses) and where n denotes the number of ground state helium atoms in the helium droplet ($n \geq 1.8 \times 10^5$):[23]

(a) $e^- + n\ He(1s^2\ ^1S) \rightarrow e^- + He(1s2p\ ^3P) + (n-1)\ He(1s^2\ ^1S) \rightarrow He(1s2s2p\ ^4P) + (n-1)\ He(1s^2\ ^1S)$ (21.9−22.9 eV)

(b) $e^- + n\ He(1s^2\ ^1S) \rightarrow e^- + He(1s3s\ ^3P) + (n-1)\ He(1s^2\ ^1S) \rightarrow He(1s2s2p\ ^4P) + (n-1)\ He(1s^2\ ^1S)$ (23.7−24.7 eV)

(c) $e^- + n\ He(1s^2\ ^1S) \rightarrow e^- + He(1s2p\ ^3P) + (n-1)\ He(1s^2\ ^1S) \rightarrow e^- + He_2(1\sigma_g^2 1\sigma_u 1\pi_u\ ^3\Pi_g) + (n-2)\ He(1s^2\ ^1S) \rightarrow e^- + He_2(1\sigma_g^2 1\sigma_u 2\sigma_g\ ^3\Sigma_u^+) + (n-2)\ He(1s^2\ ^1S) \rightarrow He_2(1\sigma_g^2 1\sigma_u 2\sigma_g 1\pi_u\ ^4\Pi_g) + (n-2)\ He(1s^2\ ^1S)$ (21.9−22.9 eV)

(d) $e^- + n\ He(1s^2\ ^1S) \rightarrow e^- + He(1s3p\ ^3P) + (n-1)\ He(1s^2\ ^1S) \rightarrow e^- + He_2(1\sigma_g^2 1\sigma_u 2\pi_u\ ^3\Pi_g) + (n-2)\ He(1s^2\ ^1S) \rightarrow e^- + He_2(1\sigma_g^2 1\sigma_u 2\sigma_g\ ^3\Sigma_u^+) + (n-2)\ He(1s^2\ ^1S) \rightarrow He_2(1\sigma_g^2 1\sigma_u 2\sigma_g 1\pi_u\ ^4\Pi_g) + (n-2)\ He(1s^2\ ^1S)$ (24.0−25.0 eV)

The formation of molecular helium anions thus appears to require first the excitation of atomic helium into a higher excited triplet state involving an orbital apart from s-symmetry at least. Subsequently, this is followed by the formation of an excited molecular helium state, which might then decay into lowest lying triplet state. Finally, capture of the free electron due to the small yet nonzero electron affinity results in the molecular helium anion. In contrast, formation of an atomic helium anion by capture of the free electron before the excited, neutral helium molecule is formed, prevents the formation of anionic molecular helium. The requirement of the intermediate associative reaction in the molecule formation process indicates a substantially smaller abundance of molecular helium anions over atomic helium anions.

We note that the suggested appearance energies are in very good agreement with the ion resonances reported earlier;[23] see the Introduction. Moreover, the highest appearance energies for the atomic and molecular anions, i.e., 23.7−24.7 eV and 24.0−25.0 eV, respectively, fit astonishingly well to the resonances at 25.1 ± 0.5 and 24.8 ± 0.5 eV reported in the literature[23] than the previously suggested pathways incorporating preceding ionization and subsequent double-electron capture at 25.5−26.5 eV; see also Table 1.

4. CONCLUSIONS

We calculated interaction potentials between helium atoms excited to the lowest lying triplet states and ground state helium. Helium molecule formation is hindered by a barrier for the lowest of these excited configurations, i.e., excitation of an electron into the 2s orbital (and concurrent spin-flip). We have shown that barriers vanish if one electron is excited into a p-orbital perpendicular to the diatomic axis instead. Furthermore, we have demonstrated that although the barriers obtained for other states under consideration account for only a few tens of millielectronvolts, they are substantial enough to prohibit molecule formation at the low temperatures present in helium droplets. Thus, we have clarified the formation of He_2* and consequently He_2^{*-} in helium droplets and beyond which electron impact energies they should be observable in electron impact experiments. The formation of He_2^{*-} requires a multistep process necessitating the intermediate formation of excited molecular helium, which is thought to be concurrent with the immediate formation of atomic helium anions. Hence, anionic helium molecules are expected to be substantially less abundant than atomic helium anions upon sufficiently energetic electron impact on helium droplets. Nonetheless, in stark contrast to experiments lacking the liquid helium environment, He_2^{*-} formation in helium droplets does not necessitate preceding ionization of helium and subsequent double-electron capture and can occur already below the ionization energy of helium of 24.5 eV.

AUTHOR INFORMATION

Corresponding Author

*A. Mauracher: tel, +43 (0)512 507 52670; electronic mail, andreas.mauracher@uibk.ac.at.

Notes

The authors declare no competing financial interest.

†S. E. Huber: e-mail, s.huber@uibk.ac.at.

ACKNOWLEDGMENTS

The computational results presented have been achieved in part using the Vienna Scientific Cluster (VSC). This work was supported by the Austrian Ministry of Science BMWF as part of the UniInfrastrukturprogramm of the Focal Point Scientific Computing at the University of Innsbruck. S.E.H. gratefully acknowledges funding from the Austrian Science Fund (FWF) DK+ project Computational Interdisciplinary Modelling, W1227-N16. A.M. gratefully acknowledges a grant from the Nachwuchsförderung of the University of Innsbruck.

REFERENCES

(1) Toennies, J. P.; Vilesov, A. F. Superfluid Helium Droplets: A Uniquely Cold Nanomatrix for Molecules and Molecular Complexes. *Angew. Chem., Int. Ed.* **2004**, *43*, 2622−2648.

(2) Stienkemeier, F.; Lehmann, K. K. Spectroscopy and dynamics in helium nanodroplets. *J. Phys. B: At. Mol. Opt. Phys.* **2006**, *39*, R127−R166.

(3) Barranco, M.; Guardiola, R.; Hernández, S.; Mayol, R.; Navarro, J.; Pi, M. Helium Nanodroplets: an Overview. *J. Low Temp. Phys.* **2006**, *142*, 1−81.

(4) Choi, M. Y.; Douberly, G. E.; Falconer, T. M.; Lewis, W. K.; Lindsay, C. M.; Merritt, J. M.; Stiles, P. L.; Miller, R. E. Infrared spectroscopy of helium nanodroplets: novel methods for physics and chemistry. *Int. Rev. Phys. Chem.* **2006**, *25*, 15−75.

(5) Yang, S.; Ellis, A. M. Helium droplets: a chemistry perspective. *Chem. Soc. Rev.* **2013**, *42*, 472−484.

(6) Pobell, F. *Matter and Methods at Low Temperatures*; Springer-Verlag: Berlin, 1996.

(7) Cencek, W.; Jeziorska, M.; Bukowski, R.; Jaszunski, M.; Jeziorski, B.; Szalewicz, K. Helium Dimer Interaction Energies from Gaussian Geminal and Orbital Calculations. *J. Chem. Phys.* **2004**, *108*, 3211−3224.

(8) Maris, H. J. Electrons in Liquid Helium. *J. Phys. Soc. Jpn.* **2008**, *77*, 111008.

(9) Wei, W.; Xie, Z.-L.; Seidel, G. M.; Maris, H. J. Experimental Investigation of Exotic Negative Ions in Superfluid Helium. *J. Low Temp. Phys.* **2013**, *171*, 178−186.

(10) Doake, C. S. M.; Gribbon, P. W. F. Fast ions in liquid helium. *Phys. Lett. A* **1969**, *30*, 252−253.

(11) Poitrenaud, J.; Williams, F. I. B. Precise Measurement of Effective Mass of Positive and Negative Charge Carriers in Liquid Helium II. *Phys. Rev. Lett.* **1972**, *29*, 1230−1232.

(12) Andersen, T.; Andersen, L. H.; Bjerre, N.; Hvelplund, P.; Posthumus, J. H. Lifetime measurements of He_2^- by means of a heavy-ion storage ring. *J. Phys. B: At. Mol. Opt. Phys.* **1994**, *27*, 1135−1142.

(13) Reinhed, P.; Orbán, A.; Werner, J.; Rosén, S.; Thomas, R. D.; Kashperka, I.; Johansson, H. A. B.; Misra, D.; Brännholm, L.; Björkhage, M.; Cederquist, H.; Schmidt, H. T. Precision Lifetime Measurements of He^- in a Cryogenic Electrostatic Ion-Beam Trap. *Phys. Rev. Lett.* **2009**, *103*, 213002.

(14) Schmidt, H. T.; Reinhed, P.; Orbán, A.; Rosén, S.; Thomas, R. D.; Johansson, H. A. B.; Werner, J.; Misra, D.; Björkhage, M.; Brännholm, L.; Löfgren, P.; Liljeby, L.; Cederquist, H. The lifetime of the helium anion. *J. Phys.: Conf. Ser.* **2012**, *388*, 012006.

(15) Michels, H. H. Electronic Structure of the Helium Molecular Anion He_2^-. *Phys. Rev. Lett.* **1984**, *52*, 1413−1416.

(16) Pluta, T.; Bartlett, R. J.; Adamowicz, L. Numerical Hartree-Fock Characterization of Metastable States of the He_2^- Anion. *Int. J. Quantum Chem.: Quantum Chem. Symp.* **1988**, *22*, 225−230.

(17) Adamowicz, L.; Pluta, T. Metastable He_2^- ions formed by two-electron attachment to the excited He_2^+ $^2\Sigma_g^+$ $(1\sigma_g^2 2\sigma_g^1)$ core. *Phys. Rev. A* **1991**, *44*, 2860−2867.

(18) Bacalis, N. C.; Kmninos, Y.; Nicolaides, C. A. Toward the understanding of He_2^- excited states. *Chem. Phys. Lett.* **1995**, *240*, 172−179.

(19) Bacalis, N. C. Existence of He_2^- negative ions with two remote electrons in antibonding orbitals. *J. Phys. B: At. Mol. Opt. Phys.* **2000**, *33*, 1415−1422.

(20) Pavanello, M.; Cafiero, M.; Bubin, S.; Adamowicz, L. Accurate Born−Oppenheimer calculations of the low-lying $c^3\Sigma_g^+$ and $a^3\Sigma_u^+$ excited states of helium dimer. *Int. J. Quantum Chem.* **2008**, *108*, 2291−2298.

(21) Henne, U.; Toennies, J. P. Electron capture by large helium droplets. *J. Chem. Phys.* **1998**, *108*, 9327−9338.

(22) da Silva, F. F.; Ptásinska, S.; Denifl, S.; Gschliesser, D.; Postler, J.; Matias, C.; Märk, T. D.; Limão-Vieira, P.; Scheier, P. Electron interaction with nitromethane embedded in helium droplets: Attachment and ionization measurements. *J. Chem. Phys.* **2011**, *135*, 174504.

(23) Huber, S. E.; Mauracher, A. On the properties of charged and neutral, atomic and molecular helium species in helium nanodroplets: interpreting recent experiments. *Mol. Phys.* **2014**, *112*, 794−804.

(24) Jiang, T.; Kim, C.; Northby, J. A. Electron Attachment to Helium Microdroplets: Creation Induced Magic? *Phys. Rev. Lett.* **1993**, *71*, 700−703.

(25) Mauracher, A.; Daxner, M.; Postler, J.; Huber, S. E.; Scheier, P.; Denifl, S. *Private communication*, 2014

(26) Gspann, J. Negatively charged helium-4 clusters. *Phys. B: Condens. Matter* **1991**, *169*, 519−520.

(27) Martin, W. C. Energy Levels of Neutral Helium (^{4}He I). *J. Phys. Chem. Ref. Data* **1973**, *2*, 257−265.

(28) Brage, T.; Fischer, C. F. Autodetachment of negative ions. *Phys. Rev. A* **1991**, *44*, 72−79.

(29) Søgaard, J.; Hazell, I.; Bjerre, N.; Andersen, T. A new method for enhancing the production of the negatively charged helium dimer He_2^-. *Chem. Phys. Lett.* **1995**, *241*, 573−576.

(30) Stanton, J. F.; Bartlett, R. J. Equation of motion coupled-cluster method: A systematic biorthogonal approach to molecular excitation energies, transition probabilities, and excited state properties. *J. Chem. Phys.* **1993**, *98*, 7029−7039.

(31) Lee, T. J.; Taylor, P. R. A diagnostic for determining the quality of single-reference electron correlation methods. *Int. J. Quantum Chem.: Quantum Chem. Symp.* **1989**, *S23*, 199−207.

(32) Woon, D. E.; Dunning, T. H., Jr. Gaussian basis sets for use in correlated molecular calculations. IV. Calculation of static electrical response properties. *J. Chem. Phys.* **1994**, *100*, 2975−2988.

(33) Frisch, M. J.; Trucks, G. W.; Schlegel, H. B.; Scuseria, G. E.; Robb, M. A.; Cheeseman, J. R.; Scalmani, G.; Barone, V.; Mennucci, B.; Petersson, G. A.; et al. *Gaussian 09*, Revision D.01; Gaussian, Inc.: Wallingford, CT, 2009.

(34) Shao, Y.; Fusti-Molnar, L.; Jung, Y.; Kussmann, J.; Ochsenfeld, C.; Brown, S. T.; Gilbert, A. T. B.; Slipchenko, L. V.; Levchenko, S. V.; O'Neill, D. P.; et al. *Q-Chem*, Version 3.1; Q-Chem, Inc.: Pittsburgh, PA. 2007.

(35) Larsen, H.; Hald, K.; Olsen, J.; Jørgensen, P. Triplet excitation energies in full configuration interaction and coupled-cluster theory. *J. Chem. Phys.* **2001**, *115*, 3015−3020.

(36) Krylov, A. I. Equation-of-Motion Coupled-Cluster Methods for Open-Shell and Electronically Excited Species: The Hitchhiker's Guide to Fock Space. *Annu. Rev. Phys. Chem.* **2008**, *59*, 433−462.